Freezing of Methanol-Water Mixtures at High Pressure in a Subsurface Ocean

Andrew Dougherty, Dustin Morris, Ross Chumsky, Xiaoqi Huang
Dept. of Physics, Lafayette College

Introduction

Sub-surface oceans have been proposed to exist on many of the large icy moons of the outer solar system. The thickness of a shell and the depth of any such ocean depend on many factors, including the composition and pressure-dependent freezing points of the materials likely to be found in the ocean.
On Enceladus, the observations of water-rich plumes [1, 2, 3, 4, 5] reveal either the presence of a liquid reservoir or highly active melting. The composition of the plumes suggests a liquid reservoir [5, 6], and the measured libration is consistent with a global subsurface ocean, rather than a localized reservoir [7]. Any subsurface ocean would likely contain impurities, such as ammonia[8] and methanol, that act as powerful antifreeze compounds. Small amounts of methanol may have been detected on the surface of Enceladus [9], as well as in the plume [3]. In addition to being a powerful antifreeze, methanol could also play a role in the formation of methane hydrates [10].

Experiments

Although the effects of pressure on pure ice and pure methanol have been extensively studied, the behavior of water-methanol mixtures under pressure has not been studied as extensively. In this work, we consider the freezing behavior of methanol-water solutions at low temperatures and moderate pressures such as might be encountered in the icy moons of the outer solar system. We report measurements of the eutectic point and the liquidus points for 30 wt.% and 80 wt.% methanol-water solutions at pressures ranging from 5 to 400 MPa, using simultaneous measurements of pressure, volume, and temperature, coupled with optical images of the sample. At very high methanol concentrations, methanol exhibits multiple solid phases (α and β) and the phase behavior is quite complex, with considerable hysteresis.

Apparatus

The apparatus consists of 3 main parts: a central high-pressure fitting, known as a cross, that contains the sample fluid, an optical system for imaging the sample, and a pressure system that includes both pressure and volume sensors.

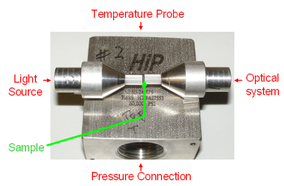

Figure 1: Exploded view of the pressure cell. Sapphire windows in steel plugs are mounted inside a steel cross. The image shows the relative positions of the plugs with windows and the plug containing the thermometer. The visible part of the sample is held in the 1 mm gap between the windows.

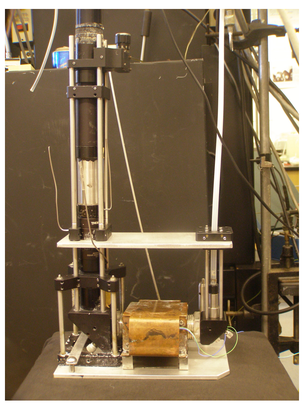

Figure 2: Optical setup surrounding the cross. Collimated light enters the pressure cell through an optical fiber on the right. The image is then relayed through a microscope objective into a CCD camera.

Methanol-Water Phase Diagram

As a methanol-water mixture is cooled, ice crystals precipitate out until the peritectic point is reached, at a temperature of approximately 171 K and a concentration of 69%, at which point $CH_3OH \cdot H_2O$ begins to form. Below the eutectic temperature of 157 K, the system solidifies completely. The eutectic concentration is approximately 88%.

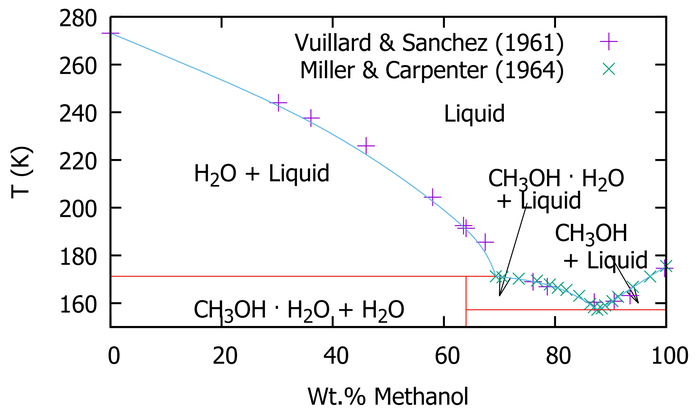

Figure 3: Atmospheric pressure phase diagram for methanol-water solutions, adapted from Kargel [11]. Data are from Vuillard & Sanchez [12] and Miller & Carpenter[13]. The current experiments have been done at concentrations of 30 wt.% and 80 wt.%.

Ice-Ih Regime

At lower pressures, less than about 200 MPa, the volume increased upon the crystallization, indicating the formation of Ice-Ih crystals. At low methanol concentrations, these ice crystals locked up the volume transducer, and it was not possible to determine the eutectic temperature accurately. We performed separate experiments at much higher methanol concentrations (80 wt.% methanol) to avoid this issue.

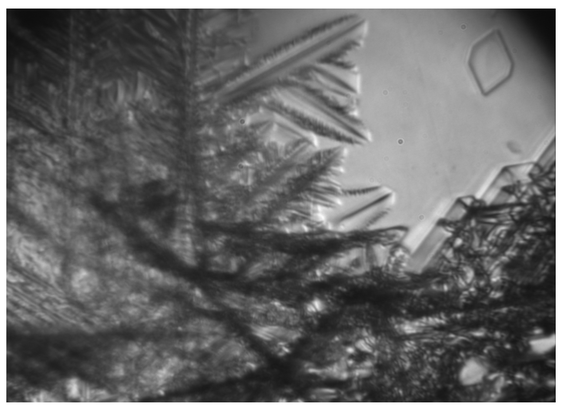

Figure 4: Ice-Ih crystals growing during the freezing of a methanol-water solution at a temperature of 254 K and pressure of 50 MPa. The image is approximately 1 mm across.

Ice-II Regime

At higher pressures, the volume decreased upon the initial crystallization of Ice crystals, indicating the formation of Ice-II.

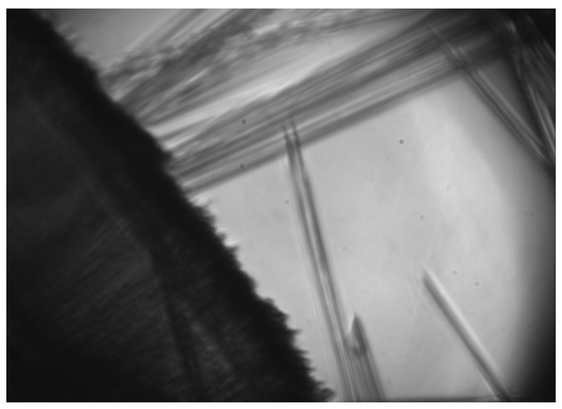

Figure 5: Image taken during the solidification of a methanol-water solution at $T = 201$ K and $p = 314$ MPa. The original thin Ice-II crystals are visible against a clear liquid background, with a solidification front approaching from the lower left-hand side of the image. The image is approximately 1 mm across.

High Pressure Crystals

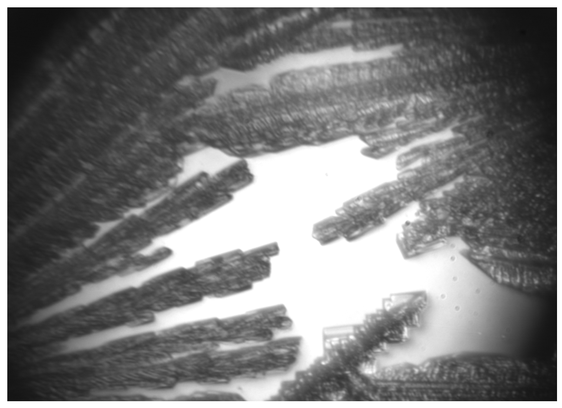

Figure 6: Crystals in a high-pressure methanol-rich solution just starting to melt at $T = 185.69$ K, $p = 201.8$ MPa. The image is approximately 1 mm across.

Results

The resulting transition temperatures are shown in Fig. 7. The phase boundaries for pure water[14, 15] and pure methanol[16] are included for comparison. For water-rich solutions, the liquidus trends follow that of pure water, while the eutectic points, and liquidus points for methanol-rich solutions, follow that of pure methanol.

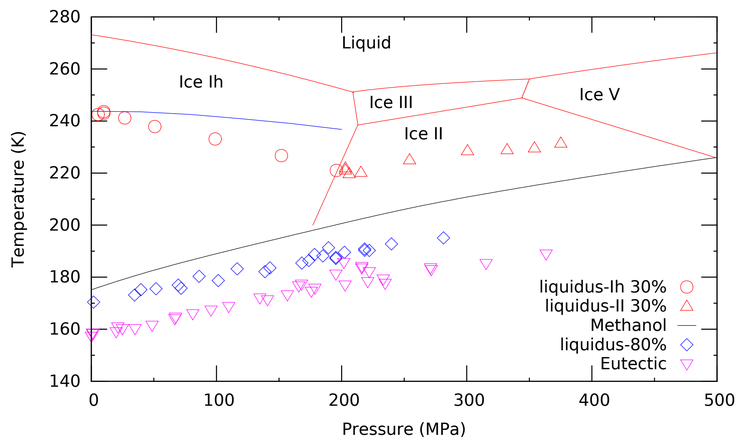

Figure 7: Transition temperatures for 30 wt.% and 80 wt.% methanol-water mixtures, with lines for water (red) and pure methanol (black) included for comparison. The blue line shows the liquidus for a 30 wt.% mixture estimated by linear interpolation between the pure ice and pure methanol curves.

Discussion

Relatively small amounts of impurities such as ammonia or methanol could have significant effects on the freezing properties of a subsurface ocean.
At the very low concentrations likely to be relevant for any subsurface ocean, the freezing point depression generally follows the ice trends, through the freezing temperature appears to decrease somewhat more rapidly with pressure than a linear interpolation between pure ice and methanol would suggest.

References

[1] M. Dougherty, et al. (2006) *Science* 311 (5766):1406. [2] C. Porco, et al. (2006) *Science* 311 (5766):1393. [3] J. H. Waite, Jr., et al. (2009) *Nature* 460 (7259):1164. [4] C. J. Hansen, et al. (2011) *Geophys Res Lett* 38:L11202. [5] H.-W. Hsu, et al. (2015) *Nature* 519 (7542):207. [6] F. Postberg, et al. (2011) *Nature* 474 (7353):620. [7] P. C. Thomas, et al. (2016) *Icarus* 264:37. [8] D. Hogenboom, et al. (1997) *Icarus* 128 (1):171. [9] R. Hodyss, et al. (2009) *Geophys Res Lett* 36:L17103. [10] G. McLaurin, et al. (2014) *Angewandte Chemie-International Edition* 53 (39):10429. [11] J. S. Kargel (1992) *Icarus* 100:556. [12] G. Vuillard, et al. (1961) *Bull Soc Chim France* 1877–1880. [13] G. A. Miller, et al. (1964) *J Chem & Eng Data* 9 (3):371. [14] W. Wagner, et al. (2011) *J Phys and Chem Ref Data* 40 (4). [15] A. N. Dunaeva, et al. (2010) *J Solar System Research* 44 (3):202. [16] A. Wurflinger, et al. (1977) *J Phys Chem Solids* 38:811.

http://sites.lafayette.edu/doughera doughera@lafayette.edu